

Establishment of a Typical Model of Parallel Ferroresonance Representation

Fathi Ben Amar

Sfax Preparatory Engineering Institute (IPEIS), University of Sfax, Tunisia.

Energy, Robotics, Control and Optimization (ERCO) Research unit of INSAT in Tunisia.

ARTICLE INFO

Article history:

Received: 13 April 2019;

Received in revised form:
10 November 2019;

Accepted: 10 November 2019;

Keywords

Parallel Ferroresonance,
Complete Model,
Reduced Model,
Temporal Comparison,
Frequency Comparison,
Typical Model.

ABSTRACT

The modeling of a parallel ferroresonant circuit leads to a single-phase model formed of many elements, which of course translates into a large number of state variables, and therefore of high dimension. We show how it is possible to gradually reduce the adopted model dimension while retaining certain characteristic quantities which seemed important for the ferroresonance study; and validate the different approximations made. Different results temporal and frequency obtained numerically on the developed models (simulating parallel ferroresonance real cases), are presented and commented. We confirm that the parallel ferroresonance is sufficiently represented qualitatively by a reduced model of dimension three.

© 2019 Elixir All rights reserved.

I. Introduction

Ferroresonance phenomena [1, 16] can occur on any electrical network having at least one capacity, interacting with a non-linear ferromagnetic element. The physical formulation of the problem results in a system of high order differential equations. For these models to be numerically integrated, it is more convenient to reduce the system order.

The object of this study is to present the physical network on which parallel ferroresonant phenomena have appeared and to try to model them by putting them in the form of a minimal order differential equations system. First, we model in detail the physical network to be studied, which is the object of this article, by decomposing it in the form of the elementary circuits (R , L and C) according to the rules used by electrical engineers. The raw model obtained leads us to work with an equations system of dimension six (6D). Then, we expose how to gradually reduce the dimension of the complete model 6D and obtain a reduced equivalent model of dimension three (3D). The idea is to eliminate the linear equations of the complete model while reducing the number of reactive elements and without modifying excessively the network global behavior. The characteristic quantities which proved to be fundamental for the appearance of parallel ferroresonant phenomena are mentioned. Finally, we validate the different approximations made, at least in the vicinity of the values of physically interesting parameters, by temporal and frequency simulations on concrete cases of parallel ferroresonance using the software matlab. The results obtained show that parallel ferroresonance is qualitatively represented by a reduced single-phase model of dimension three. In addition to limiting the number of parameters involved, this simplified model considerably reduces the calculation time. This advantage is particularly sought after in

parametric studies using numerical methods arising from bifurcation theory [4-7, 10, 11, 17].

II. Real situation of parallel ferroresonance

In voltage feedback situations, the operator is often required to switch on a unloaded transformer located at the end of a long line. The shunt capacitance constituted by the line and the non-linear inductance of the receiver transformer can cause parallel ferroresonance (figure 1) [2-5, 12, 13, 17]. This can lead to dangerous distortions and overvoltages worth several times the nominal voltage [2-7, 9-12, 17]. Any damage caused (explosion of surge arresters, transformer damage, etc.) can aggravate the situation and durably delay the service resumption.

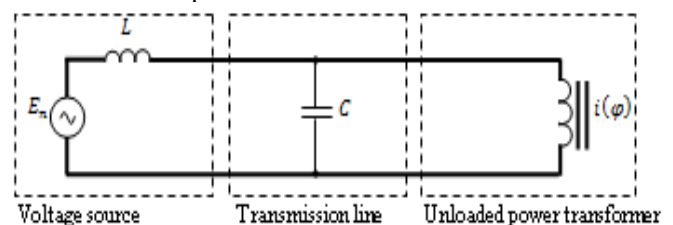


Figure 1. Parallel ferroresonance during voltage feedback operation through a long line.

The practical situations encountered are generally three-phase, but they can sometimes be represented by a single-phase network (figure 1). We encounter such a configuration in refeeding maneuvers on a very capacitive network after a generalized incident. It is this configuration that we chose to treat in this article.

III. Mathematical modeling framework

To correctly study the parallel ferroresonance phenomena by the bifurcation theory methods, we thought it important to accurately model each network part taking into account the different remarks already made on models

established in anterior works [2-4, 12-15]. Indeed, by this study, we seek to accuse the validity of these models and highlight the network parameters that seem interesting to us to represent the situations of parallel ferroresonance appearance.

The purpose of this modeling is to represent the network by a system of nonlinear ordinary differential equations, non-autonomous system, parameterized, of the form:

$$\frac{dX}{dt} = F(X, t, \lambda) \tag{1}$$

$X \in \{X_i\}$, $X \in \mathfrak{R}^n$ is the solution vector of the system whose components are the state variables (flux, voltages and currents) appearing on the network; the size of this vector depends on the modeling finesse,

$\lambda \in \mathfrak{R}^p$ is the vector containing the network parameters (line length, impedances, resistances, supply voltage, etc.),

F is a function explicitly dependent on time, because of the presence of the periodic forcing term, in sinusoidal function form.

The transformers' presence, whose characteristics are not linear, makes F non-linear with respect to its variables X_i ; which explains the appearance of unexpected phenomena on the network.

As the transient simulation times of the phenomenon are important and tedious, we have already developed in [17] a direct calculation code of the steady state without going through the calculation of the transient state by using the bifurcations theory [4-7, 17]. This computation code is based on the frequency method of Galerkin [5-7, 9, 17] and the pseudo-arclength continuation method [5-7, 17]. Both methods are satisfactory. They allow us to easily construct the bifurcation diagrams and obtain a global view of the phenomenon [4-7, 9-11, 17].

IV. Description of the voltage feedback configuration

In voltage feedback situations, the operator is forced to send back a voltage (periodic versus time) to unloaded transformer located at the end of a long line. We distinguish, then, in this system three constituent elements (Figure 2):

- the voltage source (alternator and its step-up transformer),
- the energy transmission line,
- the target transformer and its non-linear current-flux characteristic.

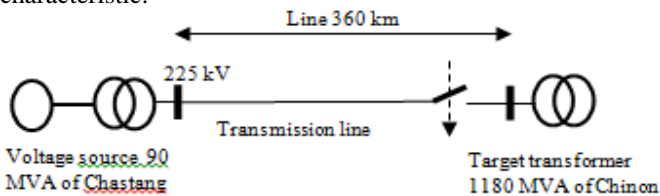


Figure 2. Example of a simplified configuration representing the voltage feedback from Chastang toward Chinon (France) [13].

As Blengino asserts [11], the real network is three-phase but the results are generally very close between phases [11-14]. That's why we chose a single-phase representation of the system considering only the direct component.

IV.1. System elements modeling

For numerical simulations to provide reliable results, a good model must be used in computational programs. To

achieve this goal, it is essential to adequately represent each component of this network. We propose here a modelization synthesis, which are also the subject of an abundant literature [9, 11-15].

IV.1.1. Voltage source model

The voltage supplied to the network comes from a source composed of an alternator accompanied by a step-up transformer (unsaturated: its characteristic is linear) (figure 3). The whole is modeled by the following single-phase element:

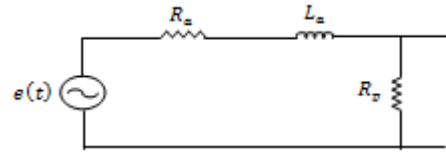


Figure 3. Voltage source model.

This representation proved sufficient during studies of ferroresonance [11, 12]. The alternator is represented by a sinusoidal e.m.f. $e(t) = E \cdot \sin(\omega t + \delta)$ located behind his subtransient reactance X_d'' increased by the leakage reactance of the source transformer X_t :

$$X_a = X_d'' + X_t \tag{2}$$

To hold into account the internal damping of the alternator's e.m.f., we associate a subtransient time constant τ'' . This damping is represented by a series resistance R_a calculated by the following relation:

$$R_a = \frac{X_d''}{\omega \tau''} \tag{3}$$

This resistance R_a is corrected from 20 Hz frequency where the skin effect begins to feel and can be deduced from its initial value by the following empirical relationship [11, 12]:

$$R_a = \frac{X_d''}{\omega \tau''} \sqrt{\frac{f}{20}} \tag{4}$$

The source characteristic values X_d'' , τ'' et X_t , provided by the manufacturers are given in percent of the basic impedance Z_n of system per-unit, often referred to as nominal impedance, defined by:

$$Z_n = \frac{U_n^2}{S_n} \tag{5}$$

with: U_n is the nominal voltage in kV,

S_n is the nominal power in MVA.

The alternator iron losses and its step-up transformer are modeled by the resistance R_p estimated on the basis of 0.2% of the nominal power S_n by the formula:

$$R_p = 100 \frac{U_n^2}{S_n} \tag{6}$$

Table 1 below gives an estimate of the parameters values of the adopted model for two sources (low and high) of nominal voltage 225 kV:

Table 1. Parameters of the voltage source model [11, 12].

S_n (MVA)	Z_n (Ω)	τ'' (ms)	X_d'' (% Z_n)	$X_d'' + X_t$ (% Z_n)	R_a (Ω)	R_p (Ω)
90	562.5	40	24	37	10.75	281250
1120	45.2	45	35.4	49	1.13	22600

This representation proved sufficient during studies of ferroresonance [11, 13]. In addition, we did not take into account the non-linearity of the unloaded alternator; the voltage remains close to the nominal voltage and the currents involved are always lower than the machine nominal current.

Similarly, Blengino has shown that the use of a more sophisticated model for the alternator and the consideration of the voltage regulator have no great influence on the results concerning ferroresonance [11].

IV.1.2. Transmission line model

We have adopted the most used model of a transmission line, namely the representation in Π given in figure 4.

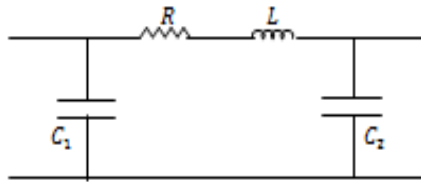


Figure 4. Transmission line model.

$C_1 = C_2 = C/2$ where C is the total capacity of the line.

In reality, a more correct representation of a long line uses a series of cells in Π (figure 4). The problem is how many cells must be considered for to have reasonable modeling. A previous study [11] shows that a modeling of the line (of length < 400 km) by several cells in Π increases the computation time without significant improvement of the results and that a representation with a cell is sufficient. Recall that the wavelength of the line at 50 Hz is about 6000 km.

The line parameters (R , L and C) will depend on the length l and will be calculated from the average lineic data from the manufacturer's abacuses [11-13].

As an example, a nominal voltage line 225 kV (50 Hz), has the following lineic characteristics:

$$R = 0.06 \Omega / km, L\omega = 0.408 \Omega / km, C = 9 nF / km$$

therefore for transmission lines whose length is between 0 and 400 km :

$$0 \leq R \leq 24 \Omega, 0 \leq L \leq 0.52 H, 0 \leq C \leq 3.6 \mu F.$$

The resistance R is calculated taking into account the skin effect from the frequency 100 Hz [11, 12].

Finally, note that a physical phenomenon can occur on the transmission line and considerably affects the network losses level: this is the crown effect. This phenomenon is related to the appearance of a conductivity of the air in the environment of a conductor brought to a high voltage. It is non-linearly dependent on voltage and frequency but, moreover, it is very sensitive to climatic conditions (rain intensity, for example), which makes it difficult to model it accurately [12].

The model adopted in our study to represent these crown losses does not take into account the nonlinear nature of the phenomenon. It is modeled, at low frequencies, by two constant resistors R_{c1} and R_{c2} in parallel with the geometric capacitances of the line [11]. It amounts to transforming the model of the line as follows (figure 5):

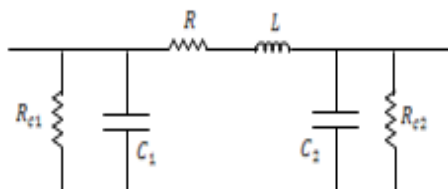


Figure 5. Final model of the transmission line

These two resistors are calculated basing on the evaluation of means crown losses. For a 225 kV network between phases, these losses are situated between 5 kW/km to 18 kW/km (from dry air to the humid air) [11, 12].

IV.1.3 Target transformer model

a. Proposed model

The transformer being empty, the adopted single-phase model is described by the figure 6 [11-13].

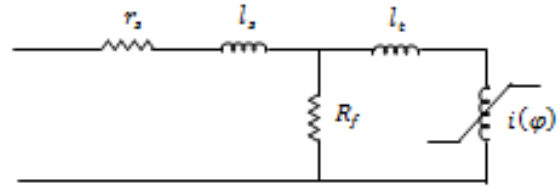


Figure 6. Target transformer model.

The resistance r_s represents the copper losses of the transformer primary. It is calculated using the following relation:

$$r_s = \frac{3P_{cc} U_n^2}{2S_n} \quad (7)$$

where P_{cc} denotes the short-circuit losses per phase of the transformer.

The ratio 1/2 comes from the fact that we consider the resistance r_s equal to 50% of the total resistance of the transformer [11, 12].

This resistance r_s is corrected taking into account the skin effect from the frequency 100 Hz [11, 12].

The linear inductance l_s is associated with the leakage flux of the transformer. It is determined by the following formula:

$$l_s \omega = \mu Z_n \quad (8)$$

with: μ is the reduced value between 10% and 15%. This quantity depends on the transformer nominal power [11, 12]; Z_n is the basic impedance defined as in (5).

The linear inductance l_l represents the saturated inductance of the transformer (equal to the self in the air of the primary winding). The corresponding reactance $l_l \omega$ is from 30% to 70% of the basic impedance [17].

b. Iron losses modeling

The iron losses in the transformer core make it possible to model the vacuum transformer more precisely, that is to say the non-linearity of the magnetising branch, taking into account the hysteresis and the eddy current losses phenomena in the circuit magnetic. In sinusoidal mode, we often choose to replace these losses by a constant resistance R_f that we can calculate by the following relation:

$$R_f = \frac{U_n^2}{3P_f} \quad (9)$$

where P_f denotes the no-load losses per phase of the transformer ;

In transient state, this model is not acceptable. A simple representation of the hysteresis phenomenon is described by a first-order nonlinear differential equation, linking the current to the flux of the form:

$$I = f(\varphi) + \frac{1}{R_f} \frac{d\varphi}{dt} \quad (10)$$

This therefore amounts to modeling the magnetizing branch of the transformer by a saturable inductance of magnetic characteristic $i(\varphi)$ associated in parallel with a

resistance of current-voltage characteristic, also non-linear, to simulate the increase of the losses iron with the voltage [11-13].

In addition, some authors neglect losses by hysteresis compared to those of eddy currents, considering that the hysteresis cycles of magnetic materials (crystal-oriented iron-silicon) used for the manufacture of transformers, are quite narrow at nominal voltage.

In [17], we have already seen that iron losses have little influence on the appearance of ferroresonance and its presence only slightly affects the value and duration of the first spikes in transient overvoltages.

c. Nonlinear inductance modeling

The function $i = f(\varphi)$ represents the non-linear characteristic of the transformer saturable inductance and plays an important role in the appearance of ferroresonant phenomena. It is about a current-flux characteristic of instantaneous values given by a series of points recorded either experimentally (rarely available) or by calculation from measurements in rms values.

For a transient simulation or the direct calculation of the steady state, we need a regular function representing this characteristic. This is why researchers have tried several approaches such as polynomial, spline and implicit functions.

The use of a polynomial function type model is justified by several authors [4-8]. It has the advantage of being easy to implement within the framework of the bifurcation theory and to give a good approximation of the phenomena. We will then adopt in our study a characteristic of the form:

$$i = f(\varphi) = k_1\varphi + k_n\varphi^n ; n \in \mathbb{N}^+ ; (k_1, k_n) \in \mathbb{R}^+ \quad (11)$$

However, it appears that we cannot represent a magnetic characteristic in the entire useful zone (saturated and unsaturated) with an expression as simple as (11). Indeed, for the strong values of the flux, it is necessary to adjust the curve $i(\varphi)$; this correction consists in considering that the iron is completely saturated and we add, in series with the nonlinear inductance, a linear inductance l_f equal to the inductance in the air of winding [11, 12].

IV.2. Complete model of System

The models presented and the remarks that we have just formulated lead to the single-phase circuit given in figure 7, representing the complete circuit for voltage feedback.

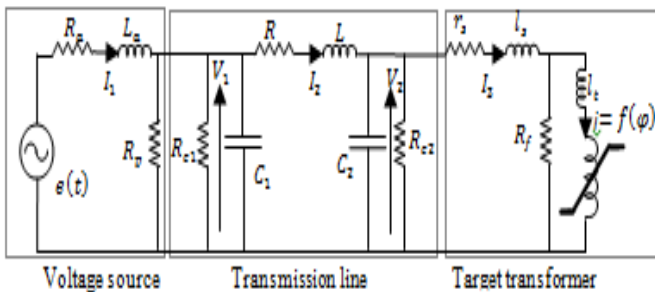


Figure 7. Complete model of voltage feedback system (of dimension 6).

The complete model obtained is made up of many elements, which naturally results in a large number of state variables, and thus differential equations.

V. Model equations and system dimension reduction

V.1. Model equations

$$\begin{cases} \dot{\varphi} = \frac{R_f(I_3 - f(\varphi))}{1 + L_f \frac{df(\varphi)}{d\varphi}} \\ L_s \dot{I}_3 = V_2 - R_f(I_3 - f(\varphi)) - r_s I_3 \\ L_a \dot{I}_1 = e(t) - V_1 - R_a I_1 \\ C_1 \dot{V}_1 = I_1 - I_2 - \frac{V_1}{R_{eq}} \quad \text{with } R_{eq} = R_p // R_{c1} \\ L \dot{I}_2 = V_1 - V_2 - R I_2 \\ C_2 \dot{V}_2 = I_2 - I_3 - \frac{V_2}{R_{c2}} \end{cases} \quad (12)$$

The state variables appearing most naturally in the circuit of figure 7 are the flux φ , the currents I_1 , I_2 and I_3 in the various inductive branches and the voltages V_1 and V_2 across the capacities. The application of the Kirchhoff laws leads to a system of 6 differential equations, parameterized, non-autonomous:

This system (12) is of dimension 6 (noted 6D). We notice that only the first two equations are nonlinear (by the presence of the term $f(\varphi)$), that the sinusoidal forcing term rendering the system non-autonomous only appears in the third equation and that the last three equations are linear. We will therefore try to eliminate these linear equations by modifying the values of the remaining parameters and obtain a model equivalent to the complete model (6D).

V.2. Reduction of the system dimension

To eliminate the linear equations of the system (12), the idea is to reduce the number of reactive elements of the model without excessively modifying the overall behavior of the network. This is done:

- by deleting certain parameters whose effect is considered weak ;
- by moving certain elements ;
- by transforming part of the network.

In our case, all the parameters appearing on the proposed model are important; we therefore choose to change the model configuration while retaining certain characteristic parameters which seemed important to us in the ferroresonance study. This amounts to transforming the element in Π (representing the transmission line) by an element in Y while retaining the characteristic properties of the circuit (figure 8).

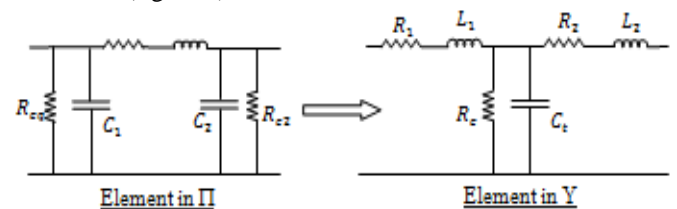


Figure 8. Switching from configuration Π to configuration Y .

In the case where the obtained mode is close to the sinusoidal mode (which is exact in the linear case), these two configurations are equivalent and we can deduce, by Kennedy's theorem, the characteristic parameters of the model (Y). These latter depend on those of the system (Pi) but are also a function of the circuit pulsation, which in our case is not constant (because of the non-linearity). We have therefore chosen, for go from the configuration (Pi) to the configuration (Y), to set four invariant quantities which are particularly important in the case of occurrence of ferroresonant

phenomena: the natural frequency of oscillation, the total capacity, the total inductance and losses.

To deduce the new parameters characteristic of the configuration (Y), we does not hold into account the losses at first (not intervening, as a first approximation, in the frequency computation), and we imposes that are preserved:

- the natural frequency seen from the nonlinear element, at the maximum of impedance :

$$\frac{1}{2\pi\sqrt{L_1 C_1}} = \frac{1}{2\pi\sqrt{L C_2}} \quad (13)$$

- the total inductance :

$$L = L_1 + L_2 \quad (14)$$

The short circuit impedance and thus preserved.

- the total capacity :

$$C_t = C_1 + C_2 \quad (15)$$

This is the impedance in open circuit that is kept.

Then, we add the losses in the same proportions (the dynamic behavior of the circuit is preserved):

- for series losses :

$$R_1 + R_2 = R \quad \text{and} \quad \frac{L_1}{R_1} = \frac{L_2}{R_2} \quad (16)$$

- for parallel losses :

$$R_e = \frac{R_{eq} \cdot R_{c2}}{R_{eq} + R_{c2}} \quad (17)$$

This allows us to reduce the number of state variables and obtain an equivalent model of dimension 4 (figure 9):

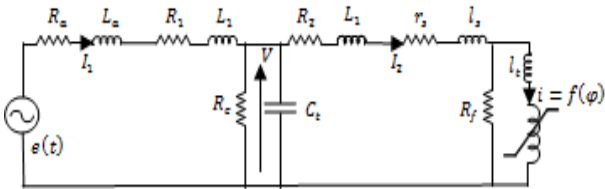


Figure 9. Model transformed 4D.

whose system of differential equations is:

$$\begin{cases} \dot{\phi} = \frac{R_f(I_2 - f(\phi))}{1 + l_1 \frac{df(\phi)}{d\phi}} \\ (L_a + L_1)\dot{I}_1 = e(t) - V - (R_a + R_1)I_1 \\ C_t \dot{V} = I_1 - I_2 - \frac{V}{R_e} \\ (L_2 + l_s)\dot{I}_2 = V - R_f(I_2 - f(\phi)) - (R_2 + r_s)I_2 \end{cases} \quad (18)$$

This system still has a linear differential equation. We then want to perform a new transformation of the previous circuit to further simplify the network studied.

Since the two resistors representing the parallel losses of the source and the target transformer (R_f and R_e) are relatively large, we decided that instead of removing them, it was preferable to move the resistor R_f to add it with the

resistor R_e . This transformation seems rather crude, but we will see later that it has little influence on the results of our study.

Thus, we obtain the simplified final model of dimension 3 (figure 10),

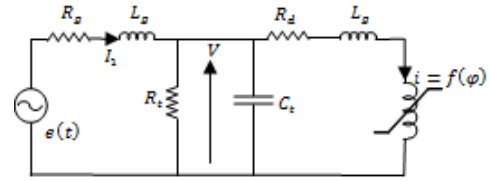


Figure 10. Final model reduced 3D.

whose equations are :

$$\begin{cases} V - R_d f(\phi) \\ \dot{\phi} = \frac{1 + l_d \frac{df(\phi)}{d\phi}}{1 + l_d \frac{df(\phi)}{d\phi}} \\ L_g \dot{I}_1 = e(t) - V - R_g I_1 \\ C_t \dot{V} = I_1 - \frac{V}{R_t} - f(\phi) \end{cases} \quad (19)$$

with:

$$\begin{cases} R_t = R_e // R_f \\ R_g = R_a + R_1 = R_a + R \frac{C_2}{C_1 + C_2} \\ L_g = L_a + L_1 = L_a + L \frac{C_2}{C_1 + C_2} \\ R_d = r_s + R_2 = r_s + R \frac{C_1}{C_1 + C_2} \\ L_d = l_s + l_1 + L_2 = l_s + l_1 + L \frac{C_1}{C_1 + C_2} \end{cases}$$

To validate the simplifications established, a comparison numerical study (temporal and frequency) of the two models 6D and 3D proves inevitable in order to know the influence of the transformations carried out on the network behavior.

VI. Validation of the reduced model

The validation interested in voltage feedback Chastang-Chinon (figure 2), where one 1180 MVA, 225 kV transformer were fed by a 90 MVA voltage source through a line of length 360 km. The non-linearity of the transformer is approximated by $i(\phi) = 2 \cdot 10^{-6} \phi + 60 \cdot 10^{-27} \phi^9$.

VI.1. Temporal comparison of different models

The temporal comparison of the two models (complete 6D and reduced 3D) will be based on a qualitative concordance (waveforms) and quantitative (maximum values) of the solution dynamics (in the transient and the steady state). To do this, a simple temporal simulation of the some typical states of the network operation is sufficient.

Table 2. Parameters and initial conditions of simulated cases of voltage feedback.

Line length	Peak source voltage	Switching instant	Remanent flux	Figure
$l = 60\text{km}$ (Short line)	$E = 30\% E_n$	$\delta = 0\text{rad}$	$\phi_r = 0\text{Wb}$	Figure 11.a
	$E = 100\% E_n$	$\delta = \pi/2\text{rad}$		Figure 11.b
		$E = 120\% E_n$	$\delta = 0\text{rad}$	$\phi_r = 40\% \varphi_n$
	$l = 360\text{km}$ (Long line)		$E = 30\% E_n$	$\delta = 0\text{rad}$
$\phi_r = 0\text{Wb}$		Figure 11.e		
$E = 100\% E_n$		$\delta = \pi/2\text{rad}$	$\phi_r = 40\% \varphi_n$	Figure 11.f
			$\phi_r = 0\text{Wb}$	Figure 11.g
$E = 120\% E_n$		$\delta = 0\text{rad}$	$\phi_r = 40\% \varphi_n$	Figure 11.h
			$\phi_r = 0\text{Wb}$	Figure 11.i
$E = 120\% E_n$	$\delta = 0\text{rad}$	$\phi_r = 0\text{Wb}$	Figure 11.j	

This numerical study consists in solving the nonlinear differential equations systems of the two models by the temporal integration step by step method, using the Runge-Kutta algorithm of order 45, with variable pitch because it seems to us to be a good compromise complexity-precision.

In a first step, we are interested in the behavior of the 6D complete model solution. Then, we study and compare the results obtained with the 3D simplified model, keeping the same conditions of study, in order to highlight the analogies and the qualitative and quantitative differences of the behavior of the two models.

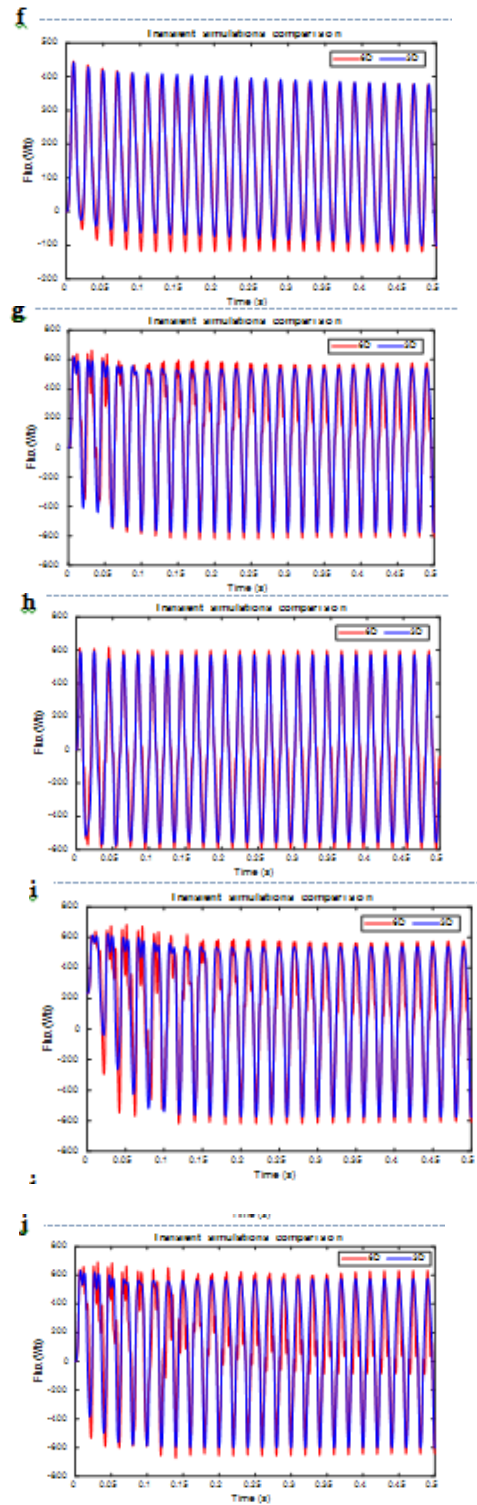
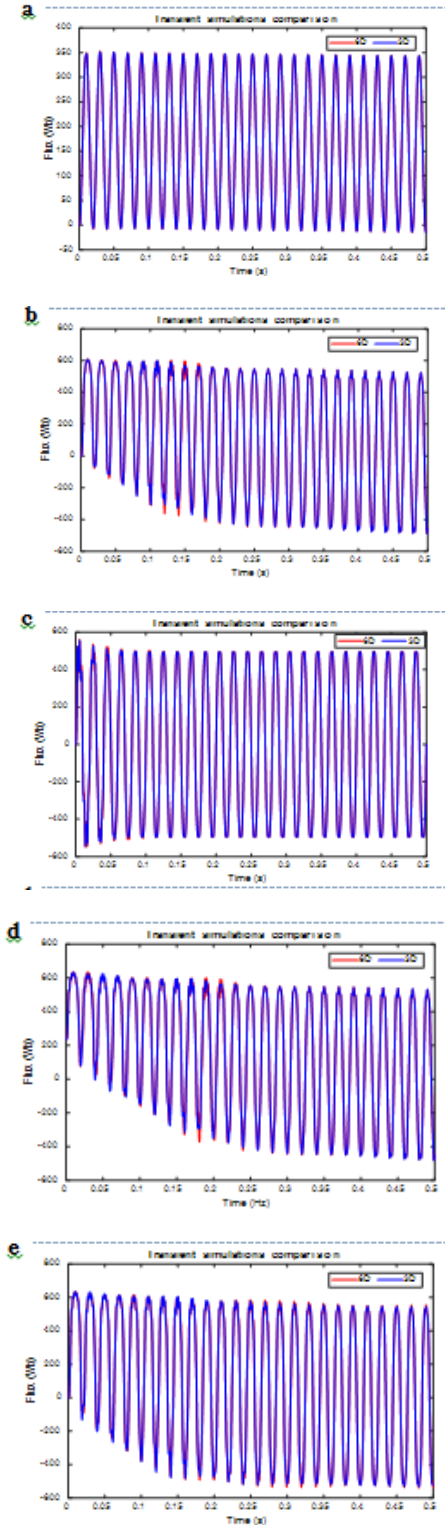


Figure 11. Temporal evolutions of flux $\varphi(t)$ in the target transformer associated to the models 6D and 3D for four cases of voltage feedback.

We therefore chose to vary mainly three parameters: the length of the transmission line, the maximal value of the applied voltage and an initial condition of the network (for example the remanent flux ϕ_r in the target transformer). The variable that seems interesting for the validation is the flux $\varphi(t)$ in the target transformer.

The initial conditions of this simulation are chosen all zero except $\varphi(0)$ which takes the value of the remanent flux ϕ_r . The latter has the effect of increasing the severity of the extreme values of the flux and to bring the target transformer into saturation; this results in an increase in harmonics and a greater risk of overvoltage.

Among many simulations performed, we show in Figure 11 a comparison of some temporal results obtained with the two models 6D and 3D for different cases of voltage feedback (Table 2).

with: $E_n = \sqrt{2/3} \cdot U_n = 183.7 \text{ kV}$ is the source voltage peak value at nominal operating and $\varphi_n = E_n / \omega = 585 \text{ Wb}$ is the flux peak value at nominal operating.

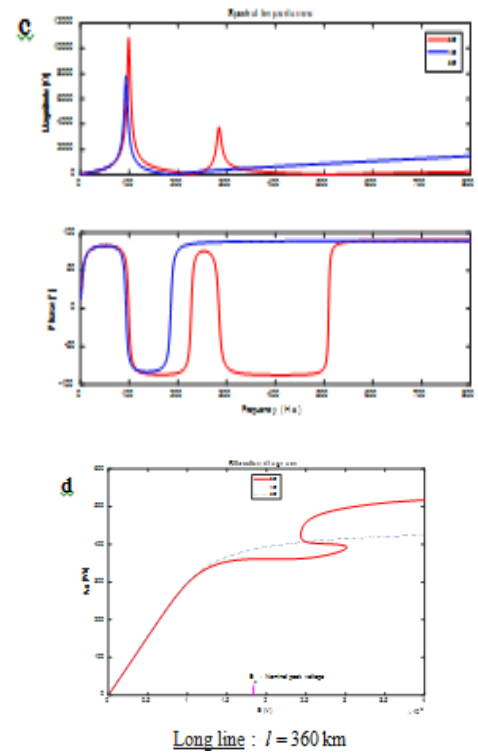
In view of the results, it can be seen that the waveforms of the temporal representations obtained with the two models 6D and 3D are quasi-similar. In fact, qualitatively, the signals dynamics are almost similar; which shows that the frequency spectra of the transient phenomena and those of the steady state are almost identical. Quantitatively, the signals are approximately equal; only a slight difference in the peak values occurs when the system becomes very capacitive (in the voltage feedback cases on the long lines).

It should be noted, however, that the temporal simulation of the 6D model is both time consuming and expensive because it requires a lot of calculation. On the other hand, the 3D model has the advantage of being as reduced as possible and quite representative of the real phenomenon; the computation time of a curve is much lower than that of the 6D model.

VI.2. Frequency comparison of different models

The frequency comparison of the 3D, 4D and 3D models will be based on a qualitative and quantitative concordance of the bifurcation diagrams of parallel ferroresonance [17]. The study is limited to reliable voltage feedback with two source machines: low of 90 MVA and high of 1120 MVA, and two line lengths: short of 50 km and 275 km long. This allows us to highlight analogies and differences in models behavior on low- and high-risk situations.

The bifurcation diagrams of the fundamental mode, as a function of the amplitude of the voltage source E (the nominal voltage between phases is $U_n = 225 \text{ kV}$), associated with the different models are given in Figures 12b, 12d, 13b and 13d.

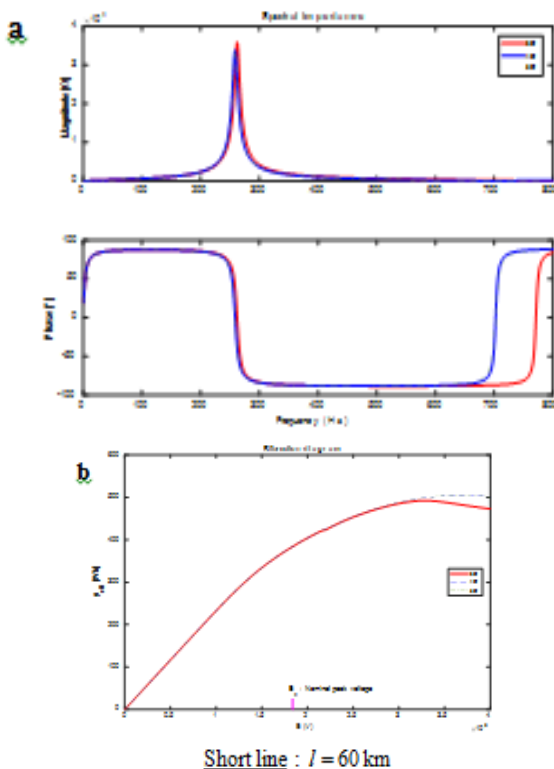


Long line : l = 360 km

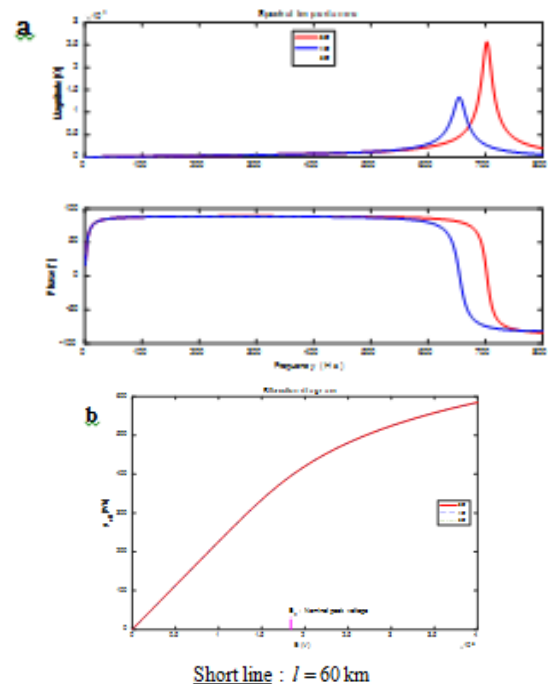
Figure 12. Network spectral impedances and bifurcation diagrams associated with different models 3D, 4D and 6D for a low source machine of 90 MVA.

We first note that the bifurcation diagrams obtained show a good qualitative and quantitative agreement between 4D and 3D models, which confirms the transition from one to the other.

On the other hand, the portion of the diagrams corresponding to the unsaturated zone of the target transformer is practically identical to that obtained with the complete model 6D, which seems normal since in linear mode (i.e. at 50 Hz), the module and argument values of the network spectral impedance for the different models are the same (see Figures 12a, 12c, 13a and 13c).



Short line : l = 60 km



Short line : l = 60 km

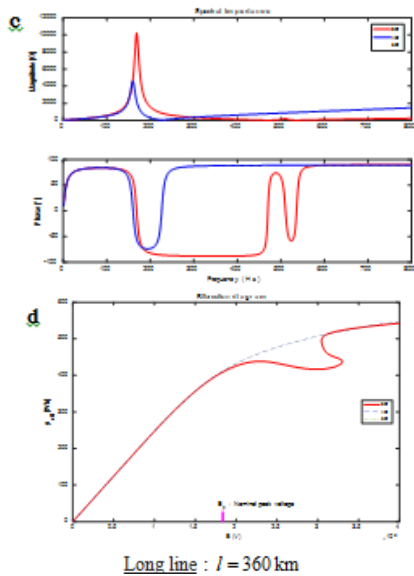


Figure 13. Network spectral impedances and bifurcation diagrams associated with different models 3D, 4D and 6D for a strong source machine of 1120 MVA.

However, in strong saturation, the bifurcation diagrams present, qualitatively, a similarity in the general form. In contrast, for extreme situations in terms of line length and the power of the voltage source, that is to say for voltage feedbacks on long lines and with a weak source machine, simple bifurcations appear on the 6D complete model while they do not exist on the 4D and 3D reduced models (Figure 12d). But from a quantitative point of view, for powerful networks (i.e. powered by strong source machines), the rms flux of the target transformer calculated by the 4D and 3D reduced models is slightly different from that calculated by the 6D model complete (Figure 13d). On the other hand, for weak and very capacitive networks (case of long lines), this difference becomes important (Figure 12d). Moreover, the critical values of the excitation voltages E corresponding to the limit-point bifurcations are visibly higher than those reached by the 6D model. Everything happens, in fact, as if we had added losses to the system.

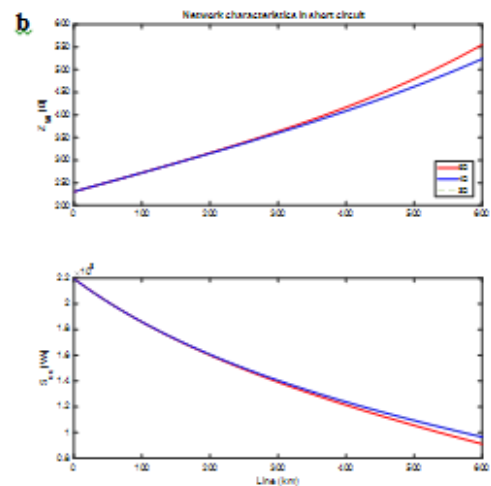
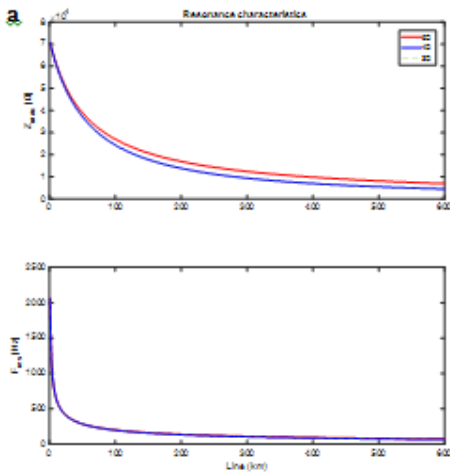
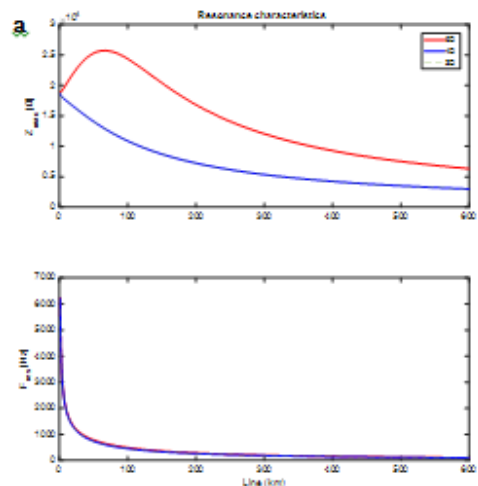


Figure 14. Resonance and short-circuit characteristics as a function of l associated with the different models 3D, 4D and 6D for a low source machine of 90 MVA.

These quantitative and qualitative differences are in fact explained by the inequality between the spectral impedances (in magnitude and in phase) of the linear circuit (network without the nonlinear element) of the three models 6D, 4D and 3D (Figures 12a, 12c, 13a and 13c). The results obtained with the two models 4D and 3D coincide perfectly and confirm the similarity of their behavior. On the other hand, this concordance is valid with the complete model 6D only for limited line lengths and bounded frequency bands. Indeed, for long lines, the behavior of these three models can be totally different. For example, for the 360 km long line and the 400 Hz frequency, the simplified models 3D and 4D have an inductive behavior; however, the complete model 6D has a capacitive behavior. This is due to the transformations used during the simplification of the modeling and is clearly visible for frequencies of rank higher than 4 (200 Hz); This is why in high saturation of the target transformer (regime rich in harmonics), one observes with the simplified models (4D and 3D) a reduction on the rms values of the flux and the absence of singularities.

Also, it is nevertheless necessary to study the characteristics of the linear network (network without the nonlinear element) in resonance (Figures 14a and 15a) and in short circuit (Figures 14b and 15b) of the three models, as a function of the line length and the power of the source machine, to ensure this equivalence in the harmonic domain. The results obtained are almost identical; which seems normal since the passage of the circuit 6D to the 3D one was made while conserving all the physical characteristics of the initial network.



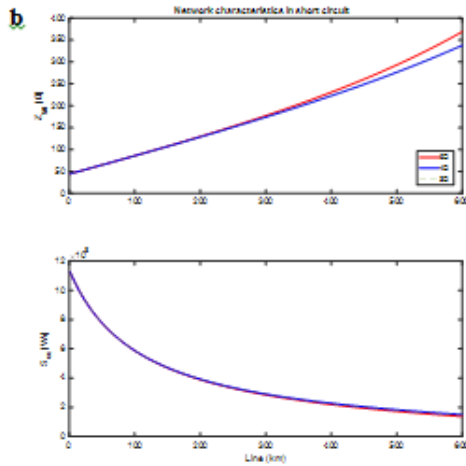


Figure 15. Resonance and short-circuit characteristics as a function of l associated with the different models 3D, 4D and 6D for a strong source machine of 1120 MVA.

Given these remarks on the different numerical results obtained with the three models, we can conclude that the 3D model is well representative of the 4D model. These simplified models are equivalent to the 6D complete model only for line lengths of a few tens of kilometers. However, in the case of very long lines, particular attention will be paid to the harmonic analysis of the models before concluding.

VII. Conclusion

In this article, we presented a modeling of a electrical system describing parallel ferroresonance. It is concluded that the raw model obtained of dimension six (6D) can be simplified and reduced to an equivalent model of dimension three (3D) sufficiently representative of the real network. It has the advantage of being the simplest theoretical case and makes it possible to bring out general conclusions relating to parallel ferroresonance.

In addition to limiting the number of parameters involved, this 3D simplified model can significantly reduce the calculation time. This advantage is particularly sought after in studies using numerical simulations in both time and frequency domains.

References

[1] G. W. Swift, "An analytical approach to ferroresonance," IEEE, Transactions on Power Apparatus and Systems, vol. Pas-88, N°1, January 1969.
 [2] S. Prusty and S. K. Sanyal, "Effect of core loss on multimodal operation of a parallel ferroresonant circuit: some generalized conclusions," IEE Proceedings, vol 126, N°92, September 1987.
 [3] G. Morin, "Service restoration following a major failure on Hydro-Quebec power system," IEEE, Transactions on Power Delivery, vol. PWRD-2, n°2, April 1987.
 [4] L. Quivy and C. Kieny, "Pseudo-periodic ferroresonant solutions stability in power network: application of bifurcation theory and Lyapunov exponents," Proceedings of the IMACS Conference (TCI'90), Nancy, France, September 1990.

[5] C. Kieny, G. Le Roy and A. Sbai, "Ferroresonance study using Galerkin method with pseudo-arclength continuation method," IEEE Transactions on Power Delivery, vol.6, N°4, October 1991.

[6] C. Kieny, "Application of the bifurcation theory for studying and understanding the global behavior of a ferroresonant electric power circuit," IEEE Transactions on Power Delivery, vol 6, N°2, April 1991.

[7] C. Kieny, A. Sbai and F. Ben Amar, "Basic principles of bifurcation applied to the study of ferroresonance," EDF Bulletin de la DER, série B, N°2, 1991, pp 69-80.

[8] T. Van Craenenbroeck, D. Van Dommelen, N. Janssens and F. Van De Meulebroeke, "Stability analysis of ferroresonant oscillations in networks with isolated neutral," IEEE International Caracas Conference on Devices, Circuits and Systems, Venezuela, December 1995.

[9] N. Janssens, Th. Van Craenenbroeck D. Van Dommelen and F. Van Meulebroeke, "Direct calculation of the stability domains of three-phase ferroresonance in isolated neutral networks with grounded-neutral voltage transformers," IEEE Transactions on Power Delivery, vol.11, N°3, July 1996.

[10] T. Van Craenenbroeck, W. Michiels, D. Van Dommelen and K. Lust, "Bifurcation analysis of three-phase ferroresonant oscillations in ungrounded power systems," IEEE Transactions on Power Delivery, vol.14, N°2, April 1999.

[11] L. Quivy, "Modélisation, analyse mathématique et simulations numériques de systèmes dynamiques complexes intervenant en ferroresonance," Thèse de Doctorat, Université de Paris-Sud (France) 1991.

[12] F. Ben Amar, A. Sbai, R. Dhifaoui and C. Kieny, "Voltage Feedback Study in Ferroresonant Electric Power Circuit: Modeling and Simulation," Conférence Internationale Francophone d'Automatique (CIFA'00), Lille, France, July 2000.

[13] M. Rioual and C. Sicre, "Energization of a no-load transformer for power restoration purposes: Impact of the sensitivity to parameters," International Conference on Power Systems Transients (IPST'01), Brazil, June 24-28 2001.

[14] Z. Emin and Yu K. Tong, "Ferroresonance experience in UK: simulations and measurements," International Conference on Power Systems Transients (IPST'01), Brazil, June 24-28 2001.

[15] S. Santoso, R. C. Dugan and P. Nedwick, "Modeling ferroresonance phenomena in an underground distribution system," International Conference on Power Systems Transients (IPST'01), Brazil, June 24-28 2001.

[16] F. Ben Amar and R. Dhifaoui, "Analytical Approach for the Systematic Research of the Periodic Ferroresonant Solutions in the Power Networks," Energy and Power Engineering, 2011, 3, 450-477.

[17] F. Ben Amar and R. Dhifaoui, "Study of the periodic ferroresonance in the electrical power networks by bifurcation diagrams," International Journal of Electrical Power & Energy Systems 33 (2011) 61-85.